

Observation of Aubry-type transition in finite atom chains via friction

Alexei Bylinskii[‡], Dorian Gangloff[†], Ian Counts and Vladan Vuletić[★]

The highly nonlinear many-body physics of a chain of mutually interacting atoms in contact with a periodic substrate gives rise to complex static and dynamical phenomena, such as structural phase transitions and friction. In the limit of an infinite chain incommensurate with the substrate, Aubry predicted a transition with increasing substrate potential, from the chain's intrinsic arrangement free to slide on the substrate, to a pinned arrangement favouring the substrate pattern¹. So far, the Aubry transition has not been observed. Here, using spatially resolved position and friction measurements of cold trapped ions in an optical lattice^{2,3}, we observed a finite version of the Aubry transition and the onset of its hallmark fractal atomic arrangement. Notably, the observed critical lattice depth for few-ion chains agrees well with the infinite-chain prediction. Our results elucidate the connection between competing ordering patterns and superlubricity in nanocontacts—the elementary building blocks of friction.

The static arrangement of a chain of interacting atoms subject to the periodic potential of a substrate lattice is governed by the competition between the associated length and energy scales: the intrinsic chain spacing competes against the lattice spacing, and the elastic energy of the chain competes against the pinning energy of the lattice potential. Aubry found a remarkable transition¹ resulting from this competition when considering an infinite chain of atoms joined by springs and subject to an incommensurate sinusoidal lattice potential (the Frenkel–Kontorova model⁴, see Fig. 1). Below a critical depth of the lattice potential U_c , chain stiffness resists pinning and favours the chain's intrinsic arrangement, resulting in a translationally invariant sliding phase. Above the critical depth, the lattice potential overcomes the stiffness of the chain, which becomes unstable against pinning. The atoms reorganize towards lattice minima and avoid lattice maxima, which become Peierls–Nabarro (PN) energy barriers. This results in analyticity breaking in the atomic positions, which form an everywhere-discontinuous fractal pattern relative to the lattice period (Fig. 1e). The critical lattice depth U_c depends on the irrational ratio of the chain-to-lattice spacing⁵ and attains its largest value at the golden ratio $\varphi = (\sqrt{5} - 1)/2$. In finite chains mismatched to the lattice, the Aubry transition takes the form of a reflection-symmetry-breaking transition^{6,7}, which in numerical simulations has appeared largely independent of chain length down to just five atoms⁷.

The problem of an atomic chain subject to a periodic potential is central to understanding nanocontacts between solids⁸ (Fig. 1a), composite materials⁹, dislocations in crystals⁴, charge density waves^{4,10}, adsorbed monolayers¹¹ and biomolecular transport¹². Realistically, those situations involve finite chains, which might additionally be attached to an external support. Furthermore, dynamical phenomena in those systems, such as friction, remain

poorly understood even at the few-atom level. In particular, stick–slip friction, the dominant mode of energy dissipation and wear at the nanoscale, originates from chain pinning, and is thought to be intimately related to Aubry's pinned phase¹³, where the force required to move the chain over the PN barriers is the friction force. Hence, below a critical lattice depth, such that PN barriers are absent, Aubry's sliding phase should manifest dynamically in smooth translation of the chain over the lattice, known as superlubricity¹³—nearly frictionless transport due to vanishing stick–slip friction. Microscopic studies of friction^{14,15} have been performed experimentally with tools ranging from very sensitive nanotribology apparatuses^{16,17} to colloidal crystals in optical lattices¹⁸. Although signatures of superlubricity have been observed at the nanoscale^{19,20}, to our knowledge, a direct and quantitative connection of these observations to Aubry's sliding phase has never been established.

Following several proposals^{21–23}, we recently studied friction between chains of trapped Yb^+ ions and an optical lattice (Fig. 1b) with atom-by-atom control unavailable in condensed-matter systems^{2–3}. We showed that superlubricity can be achieved by structurally mismatching the ion chain to the optical lattice², and, studying the velocity and temperature dependence of friction³, identified a regime where stick–slip friction is minimally affected by finite temperature. In the present work, operating in the said regime, we observe a transition from superlubricity to stick–slip with increasing lattice depth (superlubricity breaking), and the accompanying formation of discontinuities in the allowed ground-state ion positions (Aubry's analyticity breaking). We show that the critical lattice depth of this transition in the few-ion chains approaches the infinite-chain result extended to include finite external confinement^{24,25}. Thus, we observe the Aubry transition in a finite system, and establish qualitatively and quantitatively that the Aubry transition and the onset of stick–slip friction represent static and dynamic aspects, respectively, of the same physical phenomenon.

In our system^{2,26,27}, the atomic chain is a self-organized one-dimensional Coulomb crystal of laser-cooled $^{174}\text{Yb}^+$ ions spaced by a few micrometres in a linear Paul trap. The periodic lattice potential, with lattice constant $a = 185$ nm, results from an optical dipole force on the atoms by a standing wave of light (Fig. 1b). At finite depth U the lattice deforms the ion arrangement, specified by the position x_j of each ion j measured from the nearest lattice maximum (Fig. 1d). $x_{j,0}$ corresponds to the intrinsic (unperturbed) $U = 0$ arrangement (Fig. 1c). Although the intrinsic ion spacing d is not uniform along the chain, it can be controlled with nanometre precision by means of the Paul trap's axial confinement to match or mismatch the chain to the lattice. The chain is matched when all neighbouring ions are separated by an integer number of lattice periods $d \pmod{a} = 0$. The chain is maximally mismatched when the sum of lattice forces on the

Department of Physics, MIT-Harvard Center for Ultracold Atoms and Research Laboratory of Electronics, Massachusetts Institute of Technology, Cambridge, Massachusetts 02139, USA. [†]These authors contributed equally to this work. [‡]Present address: Department of Physics and Department of Chemistry and Chemical Biology, Harvard University, Cambridge, Massachusetts 02139, USA. *e-mail: vuletic@mit.edu

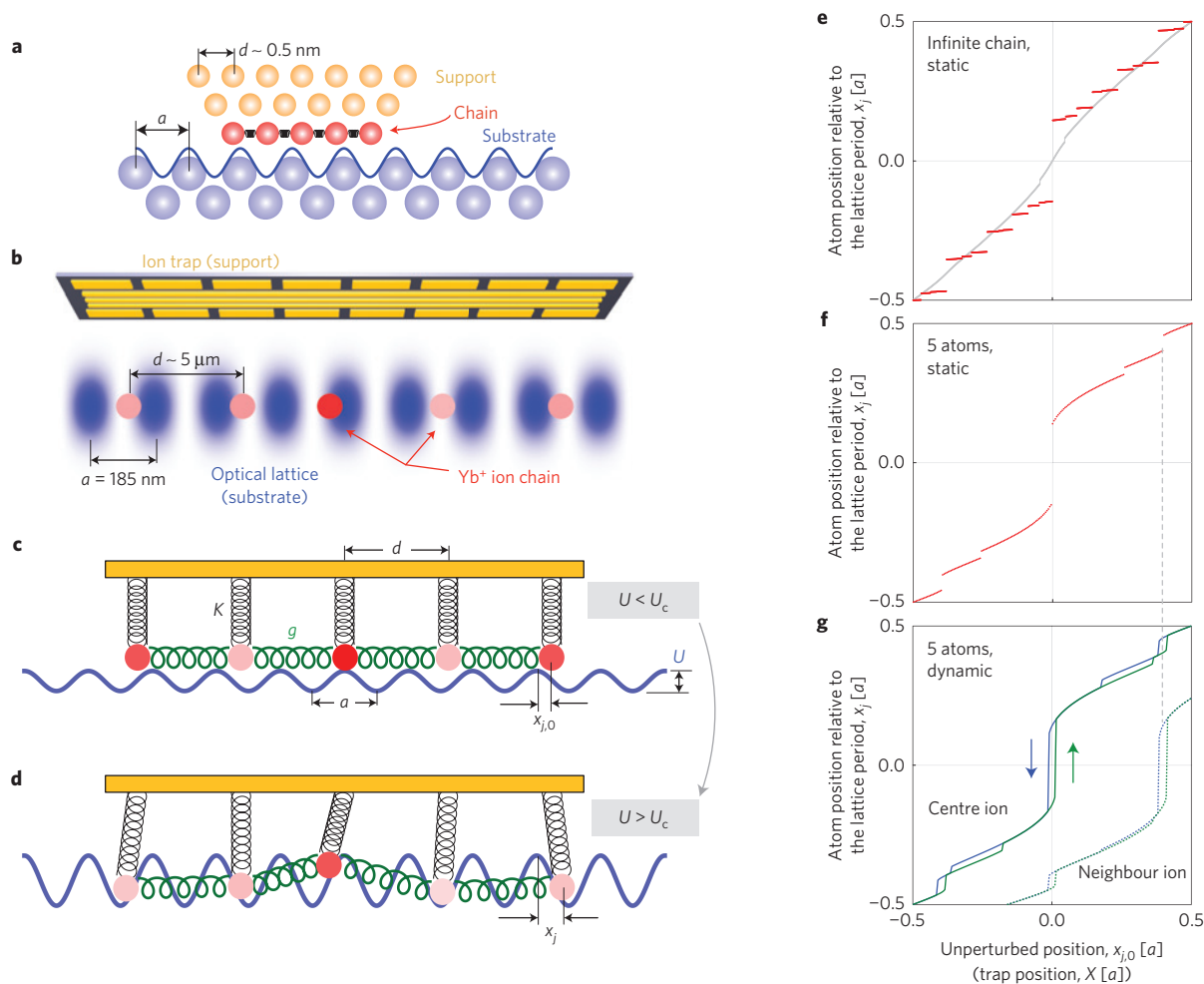


Figure 1 | A nanocontact, the ion-lattice system, the Frenkel-Kontorova-Tomlinson (FKT) model and the Aubry transition. **a**, A few-atom nanocontact modelled as a contact-layer atomic chain (red), attached to a support (yellow) and interacting with the substrate lattice via a periodic potential (blue). **b**, Our system^{2,26,27} of an ion chain trapped in a Paul trap (support) with typical axial vibrational frequency $\omega_0/(2\pi) \approx 360$ kHz and subject to an optical-lattice potential (substrate) with depth U/k_B tunable between 50 μ K and 2 mK. The ions are laser-cooled deep into the lattice to temperatures $\sim 0.05U/k_B$. Each ion's position relative to the lattice is observed by means of the position-dependent ion fluorescence arising in our laser-cooling scheme² (see Methods). **c,d**, The FKT model^{24,25} of the nanocontact (**a**) and our ion-lattice system (**b**) shown below (**c**) and above (**d**) the pinning transition. Interatomic springs of stiffness g couple neighbouring atoms in a chain of period d , while external springs of stiffness K couple them to the support. Each atom's position from the nearest lattice maximum in the absence (presence) of the lattice is given by $x_{j,0}$ (x_j). Interaction with a sinusoidal potential of depth U and period a pins the chain above a critical lattice depth U_c , resulting in avoided position regions around lattice maxima. **e**, In the limit $N \rightarrow \infty$, $K \rightarrow 0$ of the Frenkel-Kontorova model, and at $d(\text{mod } a)/a = (\sqrt{5} - 1)/2$ (the golden ratio), the curve of allowed ground-state positions x_j versus $x_{j,0}$ is continuous below the Aubry transition (grey) and forms a fractal staircase above the transition (red). (Numerical results shown are for $N = 101$ atoms and $g/K = 128$.) **f,g**, For a realistic nanocontact, for example $N = 5$, $g/K = 1$ and $d(\text{mod } a)/a = (\sqrt{5} - 1)/2$, a finite staircase forms above the transition. In a dynamical situation (fast translation of support) (**g**), the gaps in the static staircase (**f**) appear as hysteresis loops in friction measurements above the superlubricity-breaking transition. The neighbouring atom trajectory (dotted line) highlights that the secondary gaps arise from the primary instabilities of other atoms in the chain near their respective lattice maxima.

ions at their intrinsic positions $x_{j,0}$ cancels^{2,28}: $\sum_j \sin(2\pi x_{j,0} + \theta) = 0$ for any θ . This system is well described by a generalized Frenkel-Kontorova-Tomlinson (FKT) model^{24,25} of a nanocontact, involving an N -atom chain joined by interatomic springs of stiffness (spring constant) g (produced here by Coulomb forces), and attached to a rigid support by external springs of stiffness $K = m\omega_0^2$, where $\omega_0/2\pi$ is the axial common-mode vibrational frequency in the Paul trap, and m is an ion's mass (Fig. 1c). Both components of chain stiffness g and K cause resistance to deformation and pinning by the lattice when the ion chain is mismatched.

In a weak lattice, the ion chain is deformed but still continuously distributed relative to the lattice—that is, the ions assume all positions relative to the lattice as the support (Paul trap) is translated along it. In a sufficiently deep lattice, ions become pinned when they are excluded from regions near lattice maxima by its anti-confining

negative potential curvature ($2\pi^2/a^2$) U overcoming the confining total chain stiffness (g and K), and creating finite PN barriers there (Fig. 1d). This anti-confinement of a given ion near a lattice maximum, combined with interatomic forces, further excludes other ions from other lattice regions. Thus, analyticity breaking is the formation of discontinuities in the curve of an atom's position x_j versus its unperturbed position $x_{j,0}$ as the support is translated. The primary discontinuity is a gap near $x_{j,0} = 0$ from $x_j < 0$ on one side of the PN barrier to $x_j > 0$ on the other side, and progressively smaller gaps form near $x_{j,0} = d_{ij}(\text{mod } a)$ due to anti-confinement of progressively further neighbours i in the chain at intrinsic distances d_{ij} away. For a finite mismatched chain of N ions, each curve x_j should accordingly have N gaps as the support is translated by one lattice period a (Fig. 1f). In the $N = \infty$ theoretical limit, for an incommensurate chain with irrational $d(\text{mod } a)/a$,

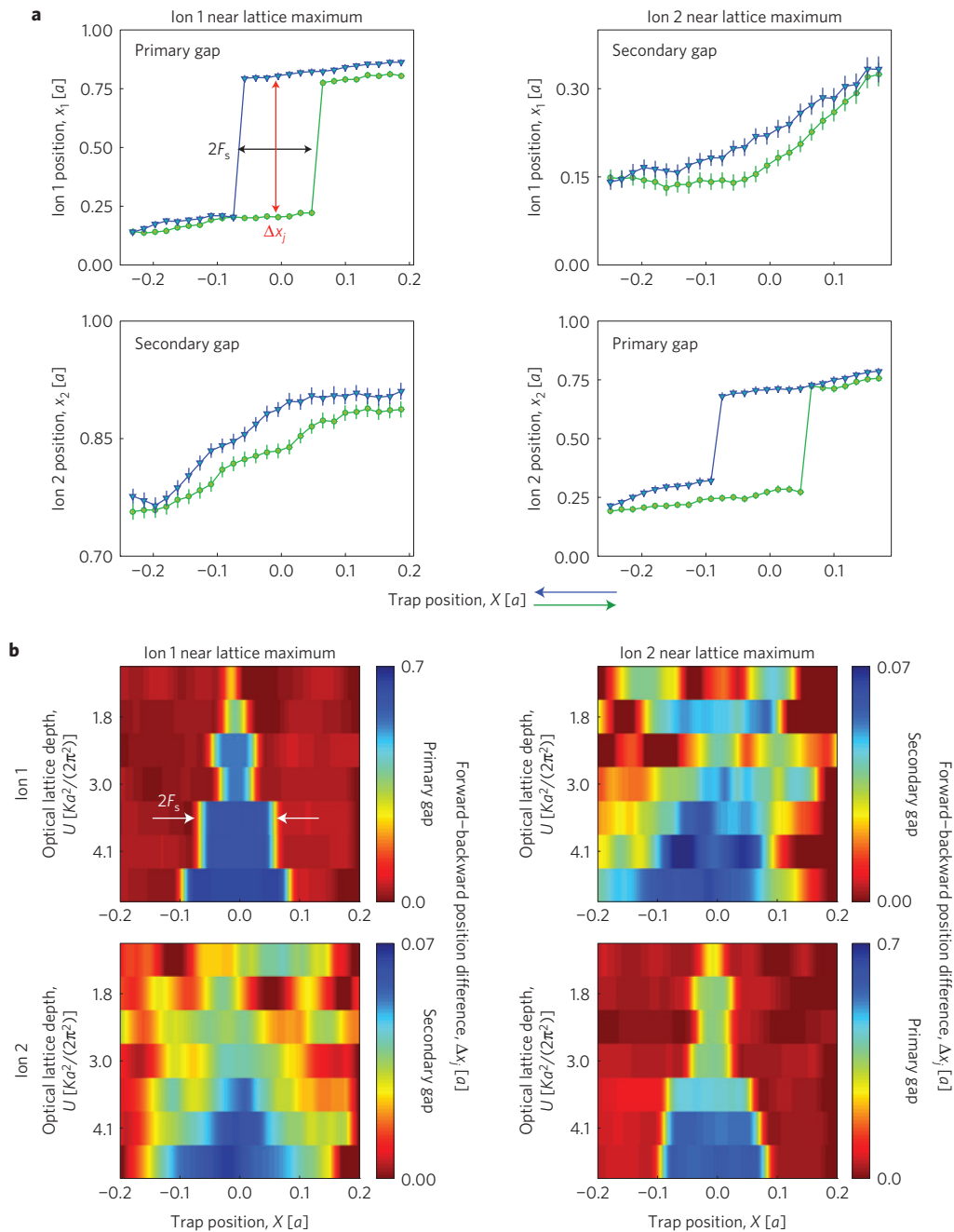


Figure 2 | Observation of primary and secondary position gap formation in a mismatched two-ion chain. a, The measured positions x_1, x_2 versus the unperturbed positions $x_{1,0}, x_{2,0}$ show both a primary hysteresis loop² for each ion, and a secondary hysteresis loop induced by the other ion's hysteresis, when the trap position X is quickly moved forwards and backwards in the vicinity of the corresponding Peierls-Nabarro barriers; here $x_{j,0}(t) = x_{j,0} + X(t)$. These loops directly reveal the gaps in each ion's ground-state position distribution. The height of each loop measures the corresponding gap, and the width of the loops measures the static friction force F_s . The two ions in this measurement are mismatched to the lattice with $d(\text{mod } a)/a \approx 2/3$. The secondary gap, corresponding to a much smaller energy scale, appears smoothed owing to finite ion temperature. The error bars show a statistical uncertainty of one standard deviation. **b**, As the lattice depth U is increased, the primary and secondary position gaps open up, as seen in the increasing difference between the forward and backward ion positions Δx_j , shown on the colour scale, and stick-slip friction sets in, as manifested by the increasing static friction force, corresponding to the half-width of the blue region $\Delta x_j > 0$. Note the different scales for the primary and secondary loops on the ion position axis in **a** and on the colour axis in **b**.

the curve of x_j (which coincides with the hull function⁴) forms a nowhere-analytic fractal staircase with an infinite number of gaps (Fig. 1e). The primary gap parameterizes the Aubry analyticity-breaking transition²⁹. In a finite chain, the primary gap for the centre ion corresponds to displacement of this ion and the chain to one side of the emerging central PN barrier, parameterizing the reflection-symmetry-breaking of the finite Aubry transition^{4,6,7,22}.

The appearance of finite PN barriers, which give rise to the gaps in the static ground-state chain arrangement at the Aubry transition, leads in the dynamic situation to stick-slip friction associated with the now bistable PN potential. Consider the ions' relative positions x_j versus the support position X (or, equivalently, versus the intrinsic positions $x_{j,0}(t) = x_{j,0} + X(t)$) when the support is moved sufficiently quickly such that the chain does not have time to thermally relax

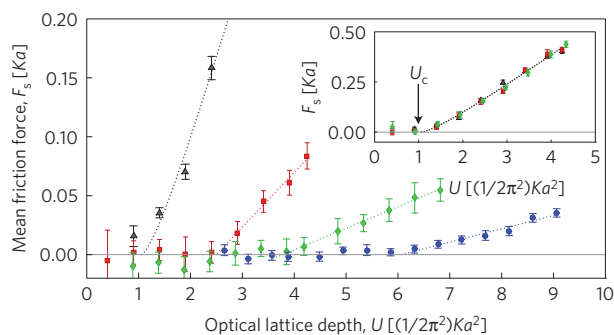


Figure 3 | Observation of superlubricity breaking for matched and mismatched ion chains. For $N=1-5$ ions matched to the lattice (inset), the measured mean friction force per ion as a function of optical lattice depth is independent of ion number, corresponding to the single-ion Prandtl–Tomlinson (PT) model (black dashed line), with superlubricity for $U < U_c = Ka^2/(2\pi^2)$; the interatomic springs g do not have any effect. For $N=1$ (black), 2 (red), 3 (green) and 5 (blue) ions mismatched to the lattice (main figure), to break superlubricity the lattice must also overcome the interatomic spring stiffness g , which increases with N , thus extending the superlubric regime to larger values of U_c . The error bars represent one standard deviation of statistical and fitting uncertainty. To extract the critical value U_c from the data, we fit an analytical formula for the PT model to the single-ion and the matched chain results (black dotted line). For the mismatched chain results, we fit a lowest-order piecewise linear model $c_0 + c_1(U - U_c)H(U - U_c)$, where H is the Heaviside step function (red, green and blue dotted lines).

across the PN barrier to the ground-state global minimum³. Then, the chain sticks to the metastable minimum below the static position gap, until the PN barrier vanishes, and a slip to the global minimum above the position gap occurs (Fig. 1g). When the support is moved in the opposite direction, the chain sticks to the metastable minimum above the position gap before slipping back to the global minimum below the position gap. This dynamical process results in hysteresis loops enclosing the gaps in the static arrangement (Fig. 1g). Below the pinning transition, there are no PN barriers: the superlubric chain always follows the global minimum and the dynamic curves of x_j coincide with the continuous static curves. Thus, the hysteresis that can be used to measure friction^{2,3} across the superlubricity-breaking transition, can also be used to measure the opening of gaps in the atomic position distribution across the analyticity-breaking transition: the two are the dynamic and static aspects, respectively, of the Aubry transition.

We perform measurements on the system by applying an external electric force F to quickly^{2,3} move back and forth the position $X(t) = F(t)/K$ of the axial trapping potential. The dynamic position curves x_j are then reconstructed from the observed ion fluorescence² (see Methods). In the elementary case of a mismatched two-ion chain we observe two hysteresis loops for each ion: a large one due to the primary slips of the ion over its lattice maximum, and a smaller one due to secondary slips induced by the primary slips of the other ion (Fig. 2a). These hysteresis loops correspond to the appearance of gaps in the allowed ion positions for the finite chain. The heights of the loops Δx_j give the desired static gaps (discontinuities) in the atomic position distribution. The left and right edges of the loops correspond to the slipping events in the stick–slip process, and the separation between them equals twice the static friction force F_s required to pull the chain over the corresponding PN barrier². The area enclosed by the loops is the energy dissipated by stick–slip in the two slip events². We observe these loops, and correspondingly the position gap Δx_j and the static friction force F_s , to grow with increasing lattice depth (Fig. 2b) as a result of growing PN barriers.

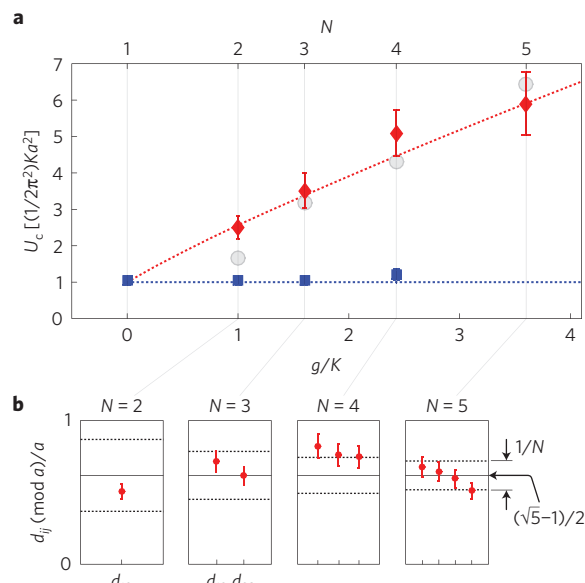


Figure 4 | Aubry transition in finite mismatched ion chains. **a**, The measured critical value U_c at the chain centre is plotted against the interatomic spring stiffness g normalized to the fixed external spring stiffness K ($\sim 1.5 \times 10^{-12}$ N m⁻¹). Each value of g/K is obtained at a different ion number N plotted on the second horizontal axis at the top. In the matched case (blue filled squares), regardless of ion number or interatomic spring stiffness, the critical lattice depth is given by the PT limit $U_c = Ka^2/(2\pi^2)$ (blue dotted line). In the mismatched case (red filled diamonds), the critical lattice depth follows the Aubry transition ($N = \infty$, $d(\text{mod } a)/a = (\sqrt{5} - 1)/2$), modified^{24,25} by the finite external confinement K (red dotted line). The grey filled circles are zero-temperature numerical simulations of our finite, inhomogeneous system with Coulomb interactions. The error bars represent a $\pm 12\%$ systematic uncertainty in applying the lowest-order fitting model to extract U_c from the data. **b**, Measured neighbour distances along each of the mismatched chains used in **a**. The distances are inhomogeneous owing to the harmonic confinement of the Coulomb chain (see Supplementary Information) and owing to a 1%-scale asymmetry of the harmonic trap. Despite these effects, the neighbour distances relative to the lattice period $d_{j,j+1}(\text{mod } a)/a$ fall within $1/(2N)$ of the golden ratio $(\sqrt{5} - 1)/2$ (dotted lines). The error bars represent one standard deviation of statistical and fitting uncertainty.

For chains of $N = 1 - 5$ ions, the measured static friction force F_s reveals that the hysteresis loops open up at a finite lattice depth U_c separating an analytic ($\Delta x_j = 0$) and superlubric ($F_s = 0$) phase for $U < U_c$ from a gapped phase ($\Delta x_j > 0$) with finite friction ($F_s > 0$) for $U > U_c$ (Fig. 3). When the ions are matched to the lattice, analyticity and superlubricity are observed to break at $U_c \approx Ka^2/(2\pi^2)$ for all N (Fig. 3 inset) as in the single-atom limit of the FKT model corresponding to the Prandtl–Tomlinson model^{14,19}. Thus, for a matched chain, anti-confinement by the lattice needs to overcome only the external chain stiffness K , as the interatomic springs remain at constant length, and play no role. When the ions are mismatched to the lattice, analyticity and superlubricity are observed to break at values of $U_c > Ka^2/(2\pi^2)$ (Fig. 3) as interatomic springs of stiffness g help keep the ions near their unperturbed positions against the lattice forces in the static limit, and store some of the lattice potential energy during motion. U_c is observed to increase with ion number as a result of increasing effective interatomic spring stiffness g . This stiffness is calculated by linearizing next-neighbour Coulomb forces for small lattice-induced deformations $\delta d/d < a/d \ll 1$, and these forces increase as ion separations d decrease when more ions are loaded in the harmonic Paul trap, leading to $g/K \approx N^{1.65}/4$ at the chain centre (see Supplementary Information). Thus, in the

large- N limit, the interatomic springs dominate the chain stiffness and the pinning behaviour, and the system is well described by the Frenkel–Kontorova model²¹. In this limit, and when the chain and the substrate are maximally incommensurate at a spacing ratio $d(\text{mod } a)/a$ equal to the golden ratio φ , the Aubry transition should occur at the largest value $U_c = ga^2/(2\pi^2)$. Non-zero external confinement K of an infinite golden-ratio chain should increase this bound^{24,25} to $U_c \gtrsim (g + K)a^2/(2\pi^2)$. Although the edge ions in our finite system pin at a lower lattice depth than the centre ions (for $N > 2$) as a result of reduced chain stiffness, the pinning of the centre ions characterizes the finite-system Aubry transition^{4,6,7,22}, and we use U_c measured at the centre for the following quantitative comparison with the infinite limit.

For maximally mismatched chains of $N = 2 - 5$ ions (each N corresponding to a different g/K), the measured chain-centre values of U_c lie close to the calculated curve of U_c versus g/K for the Aubry transition in an infinite golden-ratio chain (Fig. 4a). Thus, a finite inhomogeneous chain with the unperturbed arrangement tuned to cancel the lattice forces, in its centre can reach the maximum robustness against the breaking of analyticity and superlubricity as set by an infinite, maximally incommensurate chain. This lattice force cancellation exists for multiple arrangements²⁸, which for a uniformly spaced chain correspond to $d(\text{mod } a)/a = j/N$, where $j = 1, \dots, N - 1$. If the fraction j/N is irreducible, the finite system may be considered pseudo-incommensurate in the sense that the unit cell is the size of the system and the lattice forces on different atoms do not repeat. The PN barriers and the pinning are minimized for those pseudo-incommensurate arrangements where atoms close to each other experience dissimilar forces—a property optimized by the golden-ratio spacing in the infinite limit (see Supplementary Information). For a finite uniform chain, the smallest difference $|j/N - \varphi|$ between a pseudo-incommensurate arrangement and the golden ratio scales as $1/N$. Although our chain spacing is non-uniform, for each N in Fig. 4a we choose the arrangement closest to the golden-ratio-like pseudo-incommensurate arrangement and find that the intrinsic separations between neighbouring ions $d_{ij+1}(\text{mod } a)/a$ indeed fall within $1/(2N)$ of the golden ratio (Fig. 4b).

In summary we observe, with atom-by-atom control, the transition from superlubricity to stick–slip and from continuous to gapped position distributions in finite chains of atoms as a function of increasing interaction with a periodic substrate. We establish the connection between this transition, relevant for the interaction of real surfaces governed by finite-size nanocontacts, and Aubry's theoretical concept of analyticity breaking in infinite chains. Furthermore, quantum tunnelling of ions through the lattice, realizable in our system, could lead to a quantum-mechanical picture of friction, possibly relevant at the nanoscale and at cold surfaces. Furthermore, in a deformable optical lattice³⁰, Peierls transition physics could be studied, potentially elucidating the effects of tunnelling on charge density wave depinning¹⁰.

Methods

Methods and any associated references are available in the [online version of the paper](#).

Received 22 October 2015; accepted 16 February 2016;
published online 21 March 2016

References

- Aubry, S. The twist map, the extended Frenkel–Kontorova model and the Devil's staircase. *Physica D* **7**, 240–258 (1983).
- Bylinskii, A., Gangloff, D. & Vuletić, V. Tuning friction atom-by-atom in an ion-crystal simulator. *Science* **348**, 1115–1119 (2015).
- Gangloff, D., Bylinskii, A., Counts, I., Jhe, W. & Vuletić, V. Velocity tuning of friction with two trapped atoms. *Nature Phys.* **11**, 915–919 (2015).

- Braun, O. M. & Kivshar, Y. S. *The Frenkel–Kontorova Model: Concepts, Methods, and Applications* (Springer, 2004).
- Biham, O. & Mukamel, D. Global universality in the Frenkel–Kontorova model. *Phys. Rev. A* **29**, 5326–5335 (1989).
- Sharma, S., Bergersen, B. & Joos, B. Aubry transition in a finite modulated chain. *Phys. Rev. B* **39**, 6335–6340 (1984).
- Braiman, Y., Baumgarten, J., Jortner, J. & Klafter, J. Symmetry-breaking transition in finite Frenkel–Kontorova chains. *Phys. Rev. Lett.* **65**, 2398–2401 (1990).
- Mo, Y., Turner, K. T. & Szlufarska, I. Friction laws at the nanoscale. *Nature* **457**, 1116–1119 (2009).
- Ward, A. *et al.* Solid friction between soft filaments. *Nature Mater.* **14**, 583–588 (2015).
- Grüner, G. The dynamics of charge-density waves. *Rev. Mod. Phys.* **60**, 1129–1181 (1988).
- Braun, O. & Naumovets, A. Nanotribology: microscopic mechanisms of friction. *Surf. Sci. Rep.* **60**, 79–158 (2006).
- Bormuth, V., Varga, V., Howard, J. & Schäffer, E. Protein friction limits diffusive and directed movements of kinesin motors on microtubules. *Science* **325**, 870–873 (2009).
- Shinjo, K. & Hirano, M. Dynamics of friction: superlubric state. *Surf. Sci.* **283**, 473–478 (1993).
- Vanossi, A., Manini, N., Urbakh, M., Zapperi, S. & Tosatti, E. Colloquium: modeling friction: from nanoscale to mesoscale. *Rev. Mod. Phys.* **85**, 529–552 (2013).
- Krylov, S. Y. & Frenken, J. W. M. The physics of atomic-scale friction: basic considerations and open questions. *Phys. Status Solidi B* **251**, 711–736 (2014).
- Szlufarska, I., Chandross, M. & Carpick, R. W. Recent advances in single-asperity nanotribology. *J. Phys. D* **41**, 123001 (2008).
- Urbakh, M. & Meyer, E. Nanotribology: the renaissance of friction. *Nature Mater.* **9**, 8–10 (2010).
- Bohle, T., Mikhael, J. & Bechinger, C. Observation of kinks and antikinks in colloidal monolayers driven across ordered surfaces. *Nature Mater.* **11**, 126–130 (2012).
- Socoliuc, A., Bennewitz, R., Gnecco, E. & Meyer, E. Transition from stick–slip to continuous sliding in atomic friction: entering a new regime of ultralow friction. *Phys. Rev. Lett.* **92**, 134301 (2004).
- Dienwiebel, M. *et al.* Superlubricity of graphite. *Phys. Rev. Lett.* **92**, 126101 (2004).
- García-Mata, I., Zhironov, O. V. & Shepelyansky, D. L. Frenkel–Kontorova model with cold trapped ions. *Eur. Phys. J. D* **41**, 325–330 (2006).
- Benassi, A., Vanossi, A. & Tosatti, E. Nanofriction in cold ion traps. *Nature Commun.* **2**, 236 (2011).
- Pruttivarasin, T., Ramm, M., Talukdar, I., Kreuter, A. & Häffner, H. Trapped ions in optical lattices for probing oscillator chain models. *New J. Phys.* **13**, 075012 (2011).
- Weiss, M. & Elmer, F.-J. Dry friction in the Frenkel–Kontorova–Tomlinson model: static properties. *Phys. Rev. B* **53**, 7539–7549 (1996).
- Weiss, M. & Elmer, F.-J. Dry friction in the Frenkel–Kontorova–Tomlinson Model: dynamical properties. *Z. Phys. B* **69**, 55–69 (1997).
- Karpa, L., Bylinskii, A., Gangloff, D., Cetina, M. & Vuletić, V. Suppression of ion transport due to long-lived subwavelength localization by an optical lattice. *Phys. Rev. Lett.* **111**, 163002 (2013).
- Cetina, M. *et al.* One-dimensional array of ion chains coupled to an optical cavity. *New J. Phys.* **15**, 053001 (2013).
- Igarashi, M., Natori, A. & Nakamura, J. Size effects in friction of multiatomic sliding contacts. *Phys. Rev. B* **78**, 165427 (2008).
- Coppersmith, S. N. & Fisher, D. Pinning transition of the discrete sine-Gordon equation. *Phys. Rev. B* **28**, 2566–2581 (1983).
- Fogarty, T. *et al.* Nanofriction in cavity quantum electrodynamics. *Phys. Rev. Lett.* **115**, 233602 (2015).

Acknowledgements

We thank W. Jhe for helpful discussions. A.B. and D.G. acknowledge scholarship support from NSERC. This work was supported by the NSF.

Author contributions

A.B., D.G. and V.V. designed the experiments. D.G., A.B. and I.C. collected and analysed data. All authors discussed the results and contributed to the manuscript preparation.

Additional information

Supplementary information is available in the [online version of the paper](#). Reprints and permissions information is available online at www.nature.com/reprints. Correspondence and requests for materials should be addressed to V.V.

Competing financial interests

The authors declare no competing financial interests.

Methods

Position detection via fluorescence. Our dynamic position curves x_j are reconstructed from the observed ion fluorescence, which varies proportionally to the optical potential energy $(U/2)(1 + \cos(2\pi x_j))$ experienced by the ion. This is a result of our laser-cooling scheme, which uses the optical lattice to couple the vibrational levels n and $n - 2$ of the ion's quantized motion in the optical lattice well²⁶. The spatial dependence of this Raman coupling

is such that the off-resonant transition $n \rightarrow n$, which on resonance would be stronger by two orders of the Lamb–Dicke factor η ($\eta \approx 10\%$ for our system), increases from lattice node to lattice anti-node proportionally to the optical potential. The stronger this coupling is, the larger the scattered fluorescence, resulting in the position-dependent fluorescence signal, which, when time-resolved, amounts to sub-wavelength imaging of the ion's average trajectory.